First assessment of simultaneous dual isotope (^{123}I/^{99m}Tc) cardiac SPECT on two different CZT cameras: A phantom study

Tanguy Blaire, MD,[a,b,c] Alban Bailliez, MD, PhD,[a,b,c] Fayçal Ben Bouallegue, PhD,[d] Dimitri Bellevre, MD,[e] Denis Agostini, MD, PhD,[b,e] and Alain Manrique, MD, PhD[b,e]

[a] Department of Nuclear Medicine, UF 5881, Groupement des Hôpitaux de l'Institut Catholique de Lille, Lomme, France
[b] Normandie Univ, UNICAEN, Signalisation, électrophysiologie et imagerie des lésions d'ischémie-reperfusion myocardique, FHU REMOD-VHF, Caen, France
[c] Department of Nuclear Medicine, IRIS, Hôpital Privé Le Bois, Lille, France
[d] Department of Nuclear Medicine, CHU de Montpellier, Montpellier, France
[e] Department of Nuclear Medicine, CHU Cote de Nacre, Caen, France

Received Dec 5, 2016; accepted Feb 23, 2017
doi:10.1007/s12350-017-0841-z

Background. **We studied the impact of simultaneous dual-isotope acquisition on ^{123}I/^{99m}Tc mismatch assessment using two CZT cameras (DNM 530c, GE Healthcare and DSPECT, Biosensors International).**

Methods. **We used an anthropomorphic torso phantom (respectively filled with a solution of ^{123}I alone, ^{99m}Tc alone, and a mixture of ^{123}I and ^{99m}Tc) and its cardiac insert with two defects mimicking two matched and mismatched defects. Mismatch extent and reconstructed image contrast were evaluated.**

Results. **The acquisition mode (single vs dual) significantly impacted (i) ^{99m}Tc (but not ^{123}I) reconstructed segmental activities using both camera ($P < .001$), and (ii) image contrast (using ^{123}I and DNM 530c, $P < .0001$; and using both ^{123}I and ^{99m}Tc with DSPECT, $P < .0001$). However, the defect and mismatch size were not impacted by the type of acquisition. With both DNM 530c and DSPECT, Lin's concordance correlation coefficient and Bland–Altman analysis demonstrated an almost perfect concordance and agreement between single- and simultaneous dual-isotope segmental activity (^{123}I and ^{99m}Tc).**

Conclusions. **This study found no impact of the acquisition mode (single vs dual) or the type of camera (DSPECT vs DNM 530c) on ^{123}I and ^{99m}Tc defect size and mismatch, providing a new step toward simultaneous dual-isotope acquisition for combined innervation and perfusion assessment. (J Nucl Cardiol 2017)**

Key Words: CZT • DSPECT • DNM 530c • mIBG • dual isotope • mismatch

Electronic supplementary material The online version of this article (doi:10.1007/s12350-017-0841-z) contains supplementary material, which is available to authorized users.

The authors of this article have provided a PowerPoint file, available for download at SpringerLink, which summarizes the contents of the paper and is free for re-use at meetings and presentations. Search for the article DOI on http://SpringerLink.com.

Reprint requests: Tanguy Blaire, MD, Department of Nuclear Medicine, UF 5881, Groupement des Hôpitaux de ÍInstitut Catholique de Lille, Lomme, France; *ta.blaire@gmail.com*

1071-3581/$34.00

Copyright © 2017 American Society of Nuclear Cardiology.

Published online: 08 March 2017

Abbreviations	
^{123}I-mIBG	^{123}I-meta-iodobenzylguanidine
CCC	Concordance correlation coefficient
CZT	Cadmium-zinc-telluride
kCnts	Kilo-counts
ROI	Region of interest
VOI	Volume of interest

BACKGROUND

The relationships between cardiac autonomic nervous system dysfunction, cardiomyopathy, and cardiac arrhythmias have been long established.[1] Cardiac sympathetic innervation can be directly imaged with ^{123}I-meta-iodobenzylguanidine (^{123}I-mIBG), a radiolabeled norepinephrine analog[2] that reflects neuronal integrity by visualizing reuptake and retention in cardiac sympathetic terminals.[3] A large number of clinical studies have demonstrated the independent role of ^{123}mIBG imaging in prognosis assessment and risk stratification irrespective of the etiology of heart failure.[4-6] The new solid-state cardiac cameras based on cadmium-zinc-telluride (CZT) detectors offer higher photon sensitivity and spatial resolution compared with standard cameras.[7] However, only a few studies have evaluated their accuracy for myocardial sympathetic innervation imaging[8-11] and left ventricular perfusion assessment using perfusion-gated SPECT.[12-14]

Due to their dramatically increased energy resolution, these dedicated cardiac cameras potentially enable combined assessment of myocardial innervation and perfusion within a single-imaging session, and with a limited radiation burden.[15] Using successive perfusion and innervation imaging, Gimelli et al[8,9] demonstrated a correlation between the impairment of innervation, rest perfusion, and mechanical dyssynchrony. Bellevre et al[11] using ^{99m}Tc-tetrofosmin to localize the heart within the thorax, recently demonstrated the feasibility of determining the late heart-to-mediastinum ratio of ^{123}I-mIBG uptake using dual-isotope imaging with a CZT camera (DSPECT) in patients with heart failure.

Despite their increased energy resolution, the scatter fraction remains high with CZT cameras.[16] In addition, the tailing effect in the energy spectrum toward lower energies due to incomplete charge collection[17] may specifically affect count statistics with CZT cameras. These two phenomena may impact image acquisition within the ^{99m}Tc photopeak during ^{123}I/^{99m}Tc dual-isotope acquisition, further compromising the accuracy of left ventricular perfusion assessment using the ^{99m}Tc-labeled tracer. There is a lack of data about the use of CZT SPECT cameras for simultaneous assessment of left ventricular innervation and perfusion using ^{123}I/^{99m}Tc dual-isotope acquisition.

Using an anthropomorphic torso phantom with a cardiac insert, we aimed to compare cardiac dual-isotope imaging with separate ^{123}I and ^{99m}Tc acquisitions with simultaneous dual-isotope acquisitions performed using two commercially available CZT cameras, Discovery NM 530c (DNM 530c, GE Healthcare, Milwaukee, WI, USA) and DSPECT (Biosensors International, Caesarea, Israel).

METHODS

Phantom Studies

We used an anthropomorphic torso phantom (Data Spectrum, Hillsborough, NC) containing a cardiac insert (Figure 1). Two fillable defects were used inside the cardiac

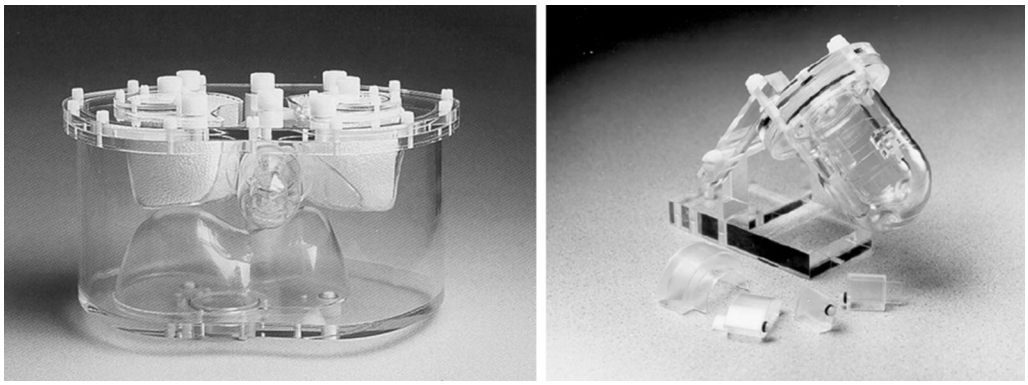

Figure 1. Anthropomorphic torso phantom (Data Spectrum, Hillsborough, NC) with two fillable cardiac defects: one (13 mL) always filled with cold water (mimicking a matched defect) and one (5.4 mL) filled with ^{99m}Tc when ^{99m}Tc solution was in the cardiac insert (mimicking a mismatched defect).

insert to mimic a matched and a mismatched defect, respectively, in the septum and the lateral wall. The phantom was successively filled with a solution of ^{123}I alone, ^{99m}Tc alone, and a mixture of ^{123}I and ^{99m}Tc. The characteristics and activities of each cardiac phantom are presented in Table 1. The liver and mediastinum compartments were filled with ^{123}I and/or ^{99m}Tc solutions as previously described.[18] Radioactivity concentrations were chosen to mimic known myocardial activities of ^{123}I-mIBG and ^{99m}Tc-tetrofosmin. Three datasets (single ^{123}I, single ^{99m}Tc, and dual ^{123}I and ^{99m}Tc) were acquired using four different acquisition times (7, 11, 22, and 33 minutes) on each camera (DNM 530c and DSPECT). In addition, a normal phantom database was built using ten single-isotope (separate ^{123}I and ^{99m}Tc) acquisitions performed with the anthropomorphic torso phantom including the cardiac insert without any defect for both cameras. The acquisition times were 5, 7, 10, 11, 12, 15, 17, 20, 22, and 33 minutes, respectively. The activities were 11 kBq/mL for ^{123}I and 22 kBq/mL for ^{99m}Tc.

CZT Cameras

We successively used (i) a DNM 530c equipped with a multiple pinhole collimator and 19 stationary CZT detectors that simultaneously image 19 cardiac views, each detector being composed of four 5-mm-thick elements of 32x32 pixels (pixel size 2.46 x 2.46 mm)[19] and (ii) a DSPECT operating with 9 mobile blocks of pixelated CZT detectors (pixel size 2.46 x 2.46 mm) associated with a wide-angle square-hole tungsten collimator, recording a total of 120 projections by each block.[16] The energy window was asymmetric for both cameras, 140 keV (−10% + 5%) for ^{99m}Tc and 159 keV (−5% + 10%) for ^{123}I, for each acquisition. No attenuation correction was performed.

Image Reconstruction

Image reconstruction was performed using dedicated commercially available software to mimic the routine clinical conditions. Scatter, crosstalk, and tailing effect were corrected using the DSPECT solely for dual (and not single)-isotope acquisitions, according to a validated method.[20] No correction was applied when using the DNM 530c. Reconstruction was performed using a specific iterative reconstruction algorithm according to each vendor's recommendation for clinical use, leading to a reconstructed pixel size of 4 x 4 x 4 and 4.92 x 4.92 x 4.92 mm, respectively, for DNM 530c and DSPECT, respectively. Short-axis reconstructed images were analyzed off-line with commercially available software[21] (QPS, Cedars-Sinai Medical Center, Los Angeles, CA), using the dedicated normal phantom databases and a 17-segment model of the left ventricle.

Image Analysis

The segmental activity (expressed in percent of the maximal myocardial activity) for ^{123}I and ^{99m}Tc in separate

Table 1. Anthropomorphic torso phantom with two fillable cardiac defects: activities for single ^{123}I (row #1), single ^{99m}Tc (row #2), and simultaneous dual ^{123}I and ^{99m}Tc acquisitions (row #3)

Phantom	Cardiac insert	Septal defect (13 mL)	Lateral defect (5.4 mL)	Liver	Mediastinum
#1	^{123}I (11 kBq/mL)	Cold water	Cold water	^{123}I (17.5 kBq/mL)	^{123}I (0.6 kBq/mL)
#2	^{99m}Tc (22 kBq/mL)	Cold water	^{99m}Tc (22 kBq/mL)	^{99m}Tc (35 kBq/mL)	^{99m}Tc (1.2 kBq/mL)
#3	^{123}I/^{99m}Tc (11/22 kBq/mL)	Cold water	^{99m}Tc (22 kBq/mL)	^{123}I/^{99m}Tc (17.5/35 kBq/mL)	^{123}I/^{99m}Tc (0.6/1.2 kBq/mL)

and simultaneous dual-isotope (^{123}I and ^{99m}Tc) acquisitions was analyzed. The results provided are related to the average of the four acquisition times.

The extent of ^{123}I and ^{99m}Tc activity defects was delineated on bull's eye polar maps using a 50% level isocontour and was quantified as a percentage of the ventricular surface. The mismatch extent was assessed as the proportion of the myocardial surface with a ^{123}I relative uptake below the 50% threshold and a ^{99m}Tc relative uptake above the 50% threshold.

Finally, contrast (%) was measured in one reconstructed midventricular small-axis slice using the imageJ software[22] by use of the count ratio (i) between the defect and the normal myocardium [Defect contrast = $100*|C_{defect} - C_{normal}|/(C_{defect} + C_{normal})$] and (ii) between the normal myocardium and the ventricular cavity [Image contrast = $100*|C_{normal} - C_{cavity}|/(C_{normal} + C_{cavity})$], where C_{defect}, C_{normal}, and C_{cavity} stand for the mean reconstructed counts in a 2 × 2-pixel region of interest (ROI), respectively, traced within the myocardial defect (septal and lateral), the normal myocardial wall, and the ventricular chamber.

Statistical Analysis

Continuous variables are presented as mean ± standard deviation (mean ± SD). The effect of camera (DNM 530c vs DSPECT), acquisition mode (single vs dual isotope), isotope (^{123}I and ^{99m}Tc), and the interaction between camera type and isotope was evaluated using a linear model analysis with a least squares fit. Concordance and agreement between single-isotope activity (separate ^{123}I and ^{99m}Tc acquisitions) and simultaneous dual-isotope activity (^{123}I and ^{99m}Tc) on DNM 530c and DSPECT were tested using Lin's concordance correlation coefficient (CCC)[23] and Bland–Altman analysis,[24] respectively. Lin's CCC is essentially equivalent to the kappa coefficient but is applicable to continuous data. It evaluates both accuracy and precision, indicating how far the measurement pairs are away from the line of identity. Paired continuous data were compared using a paired t-test. A two-tailed P value ≤ .01 was considered as statistically significant. Statistical analysis was performed using R software version 3.2.4 (R Foundation for Statistical Computing, Vienna, Austria) and JMP® version 11.0 (SAS Institute Inc., Cary, NC).

RESULTS

Assessment of Tracer Activity

The mean segmental activities obtained from single- (separate ^{123}I and ^{99m}Tc acquisitions) and simultaneous dual-isotope (^{123}I and ^{99m}Tc) acquisitions for both energy windows (^{123}I and ^{99m}Tc) are presented in Figure 2. The ^{99m}Tc activity value was significantly impacted by the acquisition mode (single vs dual) for both DNM 530c ($P < .0001$) and DSPECT ($P < .001$), but not the ^{123}I activity value (NS). Comparing the two cameras, the mean ^{123}I activity value was significantly increased using the DSPECT compared to DNM 530c with both single- ($P < .0001$) and simultaneous dual-isotope acquisition ($P < .0001$).

With both DNM 530c and DSPECT (Figure 3), Lin's CCC demonstrated an almost perfect concordance between reconstructed segmental activities from serial single-isotope and simultaneous dual-isotope acquisitions. Bland–Altman analysis confirmed the excellent agreement between single- and dual-isotope acquisitions for each camera type. When comparing the results between DNM 530c and DSPECT (Figure 4), Lin's

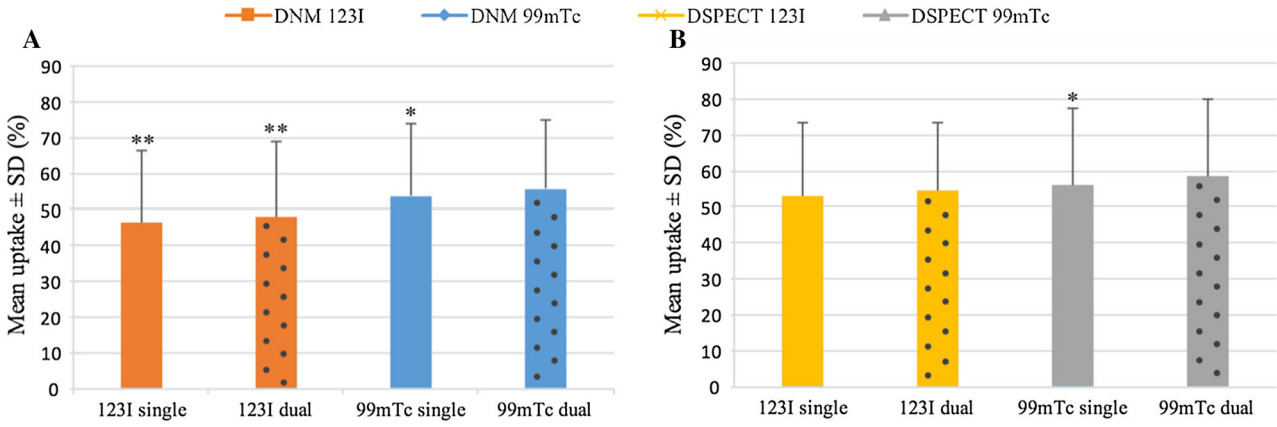

Figure 2. Segmental relative activities on DNM 530c (**A**) and DSPECT (**B**) using a 17-segment model with single (separate ^{123}I and ^{99m}Tc) acquisitions compared with simultaneous dual-isotope (^{123}I and ^{99m}Tc) acquisitions for both energy windows (^{123}I and ^{99m}Tc) expressed as mean value ± standard deviation. *$P < .001$ vs dual, **$P < .0001$ vs DSPECT.

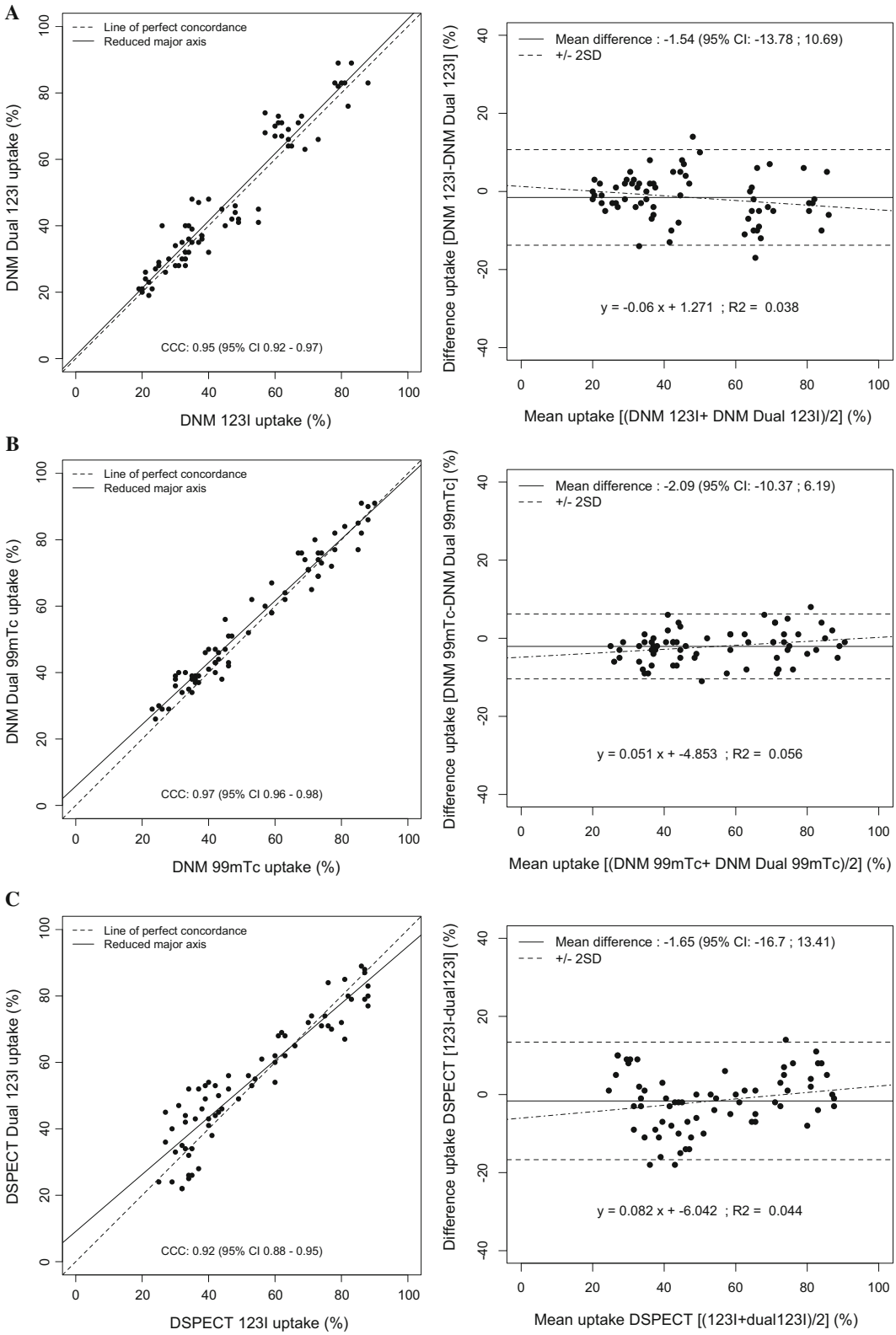

Figure 3. Lin's concordance correlation coefficients and Bland–Altman analysis for the comparison between simultaneous dual-isotope acquisition and single separate acquisition for each isotope (^{123}I and ^{99m}Tc) using DNM 530c (**A**, **B**) and DSPECT (**C**, **D**), respectively. All P values = NS.

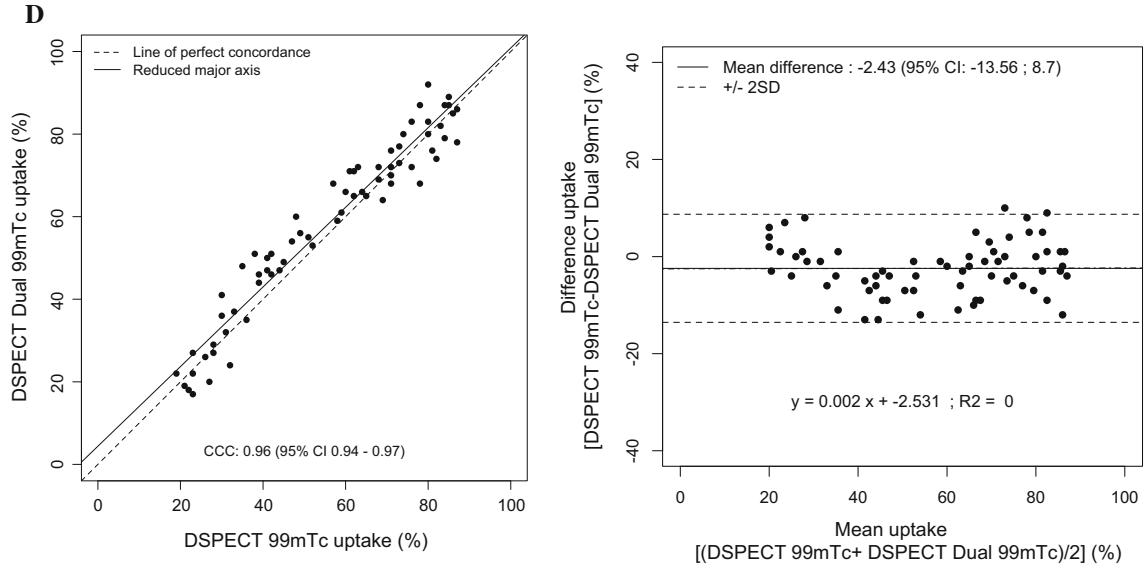

Figure 3. continued.

CCC and Bland–Altman analysis also demonstrated strong agreement between the two cameras for both single- and simultaneous dual-isotope acquisition.

Mismatch Between ^{123}I and ^{99m}Tc Activities

Defect and mismatch size delineated on bull's eye polar maps comparing single separate acquisition and simultaneous dual-isotope acquisition for each isotope (^{123}I and ^{99m}Tc) using DNM 530c and DSPECT are presented in Figure 5 and Table 2. As illustrated in Table 2, the mismatch was larger using DNM 530c compared to DSPECT. However, this difference was not statistically significant using linear model analysis that showed no impact of camera type and acquisition time on the size of activity defects and mismatch (P = NS).

Image Contrast

Image and defect contrasts comparing single- and simultaneous dual-isotope acquisition for each isotope (^{123}I and ^{99m}Tc) using both cameras are illustrated, respectively, in Figure 6A and B. As shown in Figure 6A, there was a significant decrease of ^{123}I image contrast using dual-isotope acquisition with the DNM 530c ($P < .0001$) compared to single-isotope acquisition. On the other hand, using the DSPECT, image contrast significantly increased with both ^{99m}Tc and ^{123}I using dual-isotope acquisition ($P < .0001$). However, there was no significant difference between single- and dual-isotope acquisitions regarding defect contrast for both camera and both isotope (Figure 6B, all P values = NS).

DISCUSSION

This phantom study was designed to mimic the combined evaluation of left ventricular perfusion and innervation by means of an anthropomorphic torso phantom with a cardiac insert, imaged using the two commercially available CZT cameras. Although there was a significant effect of dual-isotope acquisition on estimates of ^{99m}Tc activity, our results demonstrated that the size of both ^{123}I and ^{99m}Tc defects as well as their mismatch was impacted neither by the type of camera (DSPECT vs DNM 530c), nor by the acquisition mode (single vs dual) or by the acquisition time. To our knowledge, this is the first dual-isotope torso phantom study assessing perfusion (^{99m}Tc) and innervation (^{123}I) using two commercially available CZT cameras (DNM 530c and DSPECT). Our results also suggested that a dual ^{123}I-^{99m}Tc acquisition does not compromise the assessment of ventricular perfusion using the ^{99m}Tc photopeak in comparison with a single ^{99m}Tc acquisition.

In the clinical setting, simultaneous dual-radionuclide acquisition provides perfectly registered functional images within a reduced imaging time. Using conventional Anger cameras, several dual-radionuclide SPECT imaging protocols have been proposed. Simultaneous ^{99m}Tc-sestamibi/^{123}I-BMIPP imaging was used for

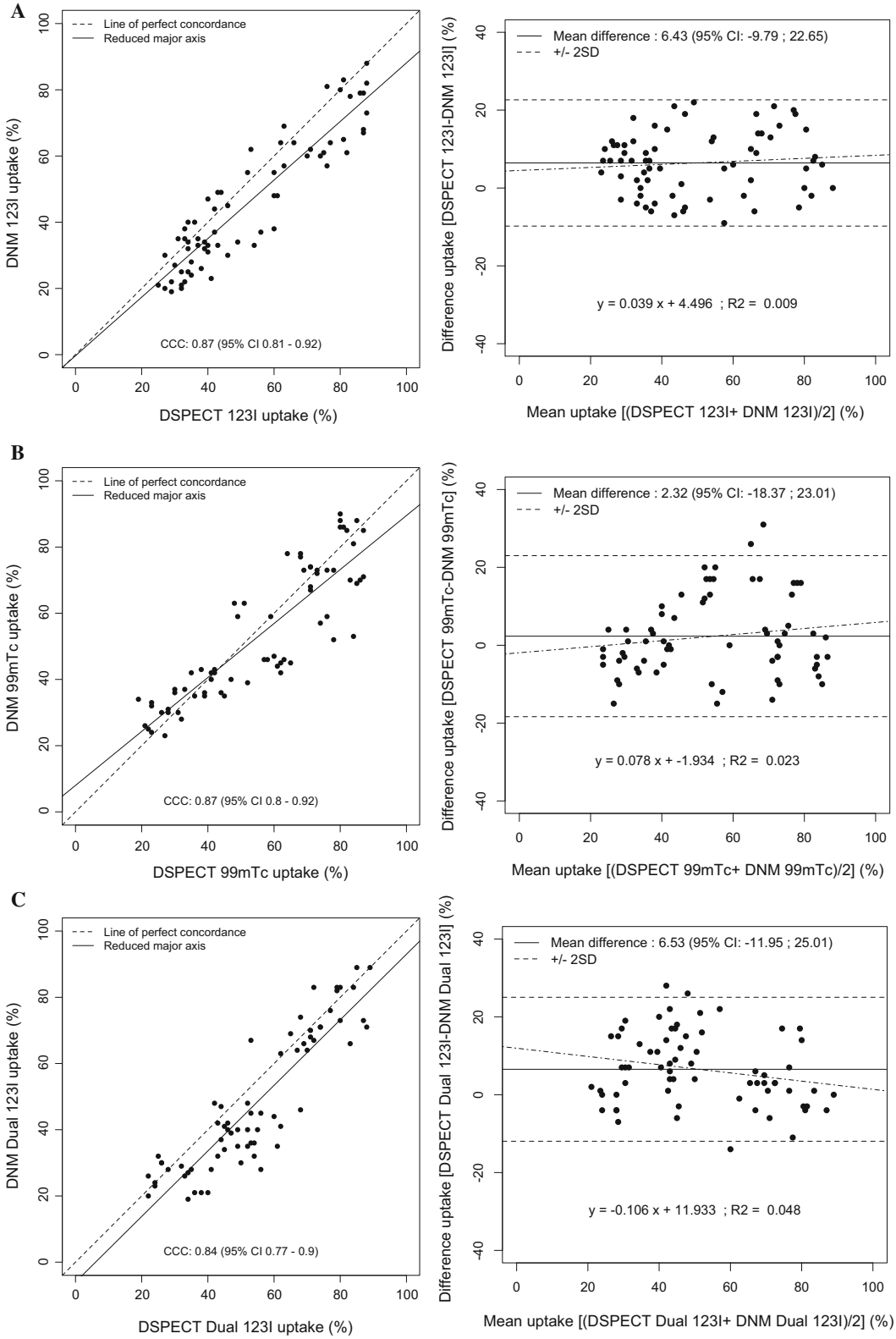

Figure 4. Lin's concordance correlation coefficients and Bland–Altman analysis for the comparison between the 2 CZT cameras for both isotope (^{123}I and ^{99m}Tc) and acquisition mode (single separate acquisitions (**A**, **B**) and simultaneous dual-isotope acquisition (**C**, **D**), respectively). All *P* values = NS.

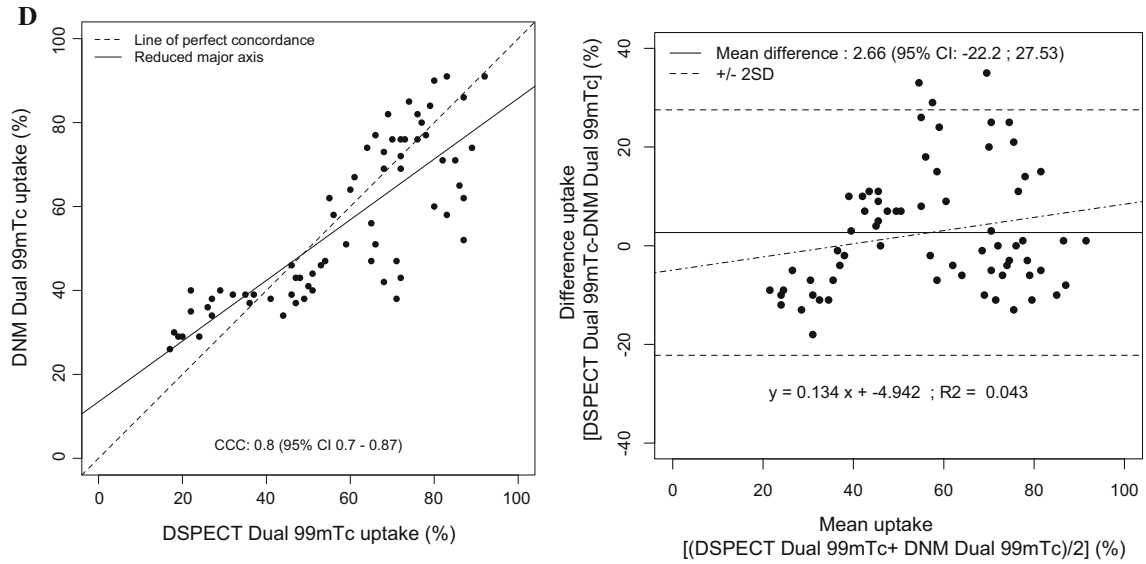

Figure 4. continued.

assessing rest perfusion and fatty acid metabolism at the same time in patients with recent myocardial infarction.[25,26] Using the conventional Anger camera, the simultaneous dual-isotope acquisition using ^{201}Tl and ^{123}I-mIBG is well documented and widely used, with possible scatter and crosstalk correction.[27] A combined perfusion and sympathetic innervation imaging with serial ^{123}I-mIBG and ^{99m}Tc-labeled tracers enables the evaluation of innervation-perfusion mismatch and may provide valuable information to assess the extension of the trigger zone as a prognostic factor of the ventricular arrhythmia in infarcted myocardium.[2,28] In addition, Gimelli et al,[8,9] using the DNM 530c camera and a sequential ^{123}I-mIBG and ^{99m}Tc-tetrofosmin myocardial SPECT, demonstrated a relevant association between innervation derangement, impaired myocardial perfusion, and mechanical dyssynchrony. Dual-isotope acquisition with CZT cameras remains a challenging technique. Impaired myocardial innervation leads to low myocardial ^{123}I-mIBG uptake, requiring a dual-isotope protocol to localize the heart.[11] Due to the small field-of-view of the dedicated CZT cardiac cameras, a scout view is mandatory to localize the heart and correctly center the field-of-view prior to SPECT acquisition. In addition, most of the patients referred for ^{123}I-mIBG assessment have an ischemic cardiomyopathy with heart failure (66% in the ADMIRE-HF study[6]). In this clinical setting, the dual-isotope protocol allows a simple and efficient co-registration of innervation and perfusion studies, and thus a robust assessment of innervation-perfusion mismatch. The measurement of myocardial innervation and perfusion is a key step of prognosis assessment and may potentially be altered when using CZT cameras with a simultaneous dual-isotope protocol due to down-scatter, crosstalk, and tailing effect of ^{123}I in the ^{99m}Tc photopeak.

Despite a significant increase in energy resolution and sensitivity, the scatter fraction remains high with CZT cameras (30% vs 34% with conventional Anger gamma cameras).[16] Due to incomplete charge collection and inter-crystal scatter, the CZT detectors are subjected to a tailing effect at the lower part of the photopeak that may lead to an over-correction of photon scatter, when using multiple energy windows methods.[20] Recently, Fan et al with a DNM 530c[29] and Holstensson et al with a DSPECT[30] presented a model-based correction algorithm which extracts the useful primary counts of ^{99m}Tc and ^{123}I from projection data, taking into account the tailing effect to correct for scatter and crosstalk in ^{99m}Tc-^{123}I dual imaging. In our study, all reconstructions were performed using the vendor's workstation and commercially available software for both cameras. Routinely, scatter, crosstalk, and tailing effect corrections[29] were not available for the DNM 530c. On the other hand, image data from DSPECT were corrected for scatter, crosstalk, and tailing effect using a previously described method.[20] The ratio between ^{123}I and ^{99m}Tc activity concentrations was set to 1:2, which is representative of the low ^{123}I-mIBG myocardial uptake observed in patients with heart failure. Under these conditions, the absence of corrections when using the DNM 530c did not affect the assessment of ^{99m}Tc defect size with simultaneous dual ^{99m}Tc-^{123}I acquisition compared to single ^{99m}Tc acquisition.

Table 2. Defect and mismatch size delineated on bull's eye polar maps using a 50% level isocontour and quantified as a percentage of the ventricular surface with single-isotope compared with simultaneous dual-isotope acquisitions for both energy windows (^{123}I and ^{99m}Tc) on DNM 530c and DSPECT

Camera	DNM 530c						DSPECT					
	Single			Dual			Single			Dual		
Acquisition type Energy window	^{123}I	^{99m}Tc	Mismatch	^{123}I	^{99m}Tc	Mismatch	^{123}I	^{99m}Tc	Mismatch	^{123}I	^{99m}Tc	Mismatch
7-Min acquisition	26	21	5	28	20	8	26	20	6	26	20	6
11-min acquisition	27	20	7	26	21	5	26	20	6	24	20	4
22-Min acquisition	27	19	8	28	19	9	27	22	5	26	20	6
33-Min acquisition	27	19	8	27	20	7	25	21	4	26	21	5
Mean ± SD (%)	26.8 ± 0.5	19.8 ± 0.9	7.0 ± 1.4	27.3 ± 0.9	20 ± 0.8	7.3 ± 1.7	26.0 ± 0.8	20.8 ± 1.0	5.3 ± 1.0	25.5 ± 1.0	20.3 ± 0.5	5.3 ± 0.9

All *P* values = NS

D'Estanque et al[31] recently reported the impact of scatter correction in dual-isotope (^{201}Tl/^{123}I-mIBG) cardiac SPECT protocols for trigger zone assessment with the DNM 530c. This correction improved the accuracy of myocardial SPECT for mapping the segmental myocardial sympathetic denervation. In their study, perfusion was assessed using Thallium, which energy window was centered at 67 keV ± 10%, right in the ^{123}I down-scatter and crosstalk window. The contribution of tailing and down-scatter photons from the photopeak of ^{123}I, detected as primary photons in the ^{99m}Tc energy window is less important than in the ^{201}Tl energy window, as depicted in Figure 7. According to D'Estanque et al, scatter correction is required when using ^{201}Tl/^{123}I-mIBG.

Although only the possible evaluation with and without scatter correction could help better understand the need or not to use scatter for the DNM 530c, our results suggest that correction for crosstalk, scatter, and tailing effect of ^{123}I in the ^{99m}Tc photopeak may likely have only limited clinical relevance in patients with ischemic heart disease.

The availability of tailing effect correction using the DSPECT camera only for dual (and not single)-isotope acquisitions[20] may explain the difference in terms of image contrast between single-isotope (separate ^{123}I and ^{99m}Tc acquisitions) and simultaneous dual-isotope (^{123}I and ^{99m}Tc) acquisitions with the DSPECT. This led to a higher image contrast for both ^{123}I and ^{99m}Tc images when using a simultaneous dual-isotope acquisition with the DSPECT compared to single-isotope acquisition. ^{99m}Tc crosstalk into the ^{123}I window is negligible when performing a simultaneous CZT acquisition.[20]

LIMITATIONS OF THE STUDY

As reconstructions were performed according to each manufacturer's recommendations, scatter, crosstalk, and tailing effect corrections were available with the DSPECT but not with the DNM 530c camera. However, our results showed no critical differences between the single- and dual-isotope conditions for the assessment of ^{99m}Tc images, even with the DNM 530c. At best, the demonstration could be made by comparing the results obtained with and without corrections.[29,30] However, the aim of our study was to compare the results obtained with the two CZT cameras using the dedicated commercially available software to mimic routine clinical conditions. Finally, our results were obtained using specific reconstruction and filtering algorithms recommended by the manufacturers for clinical use and cautions are required in case of using different algorithms in order to achieve successful assessment.

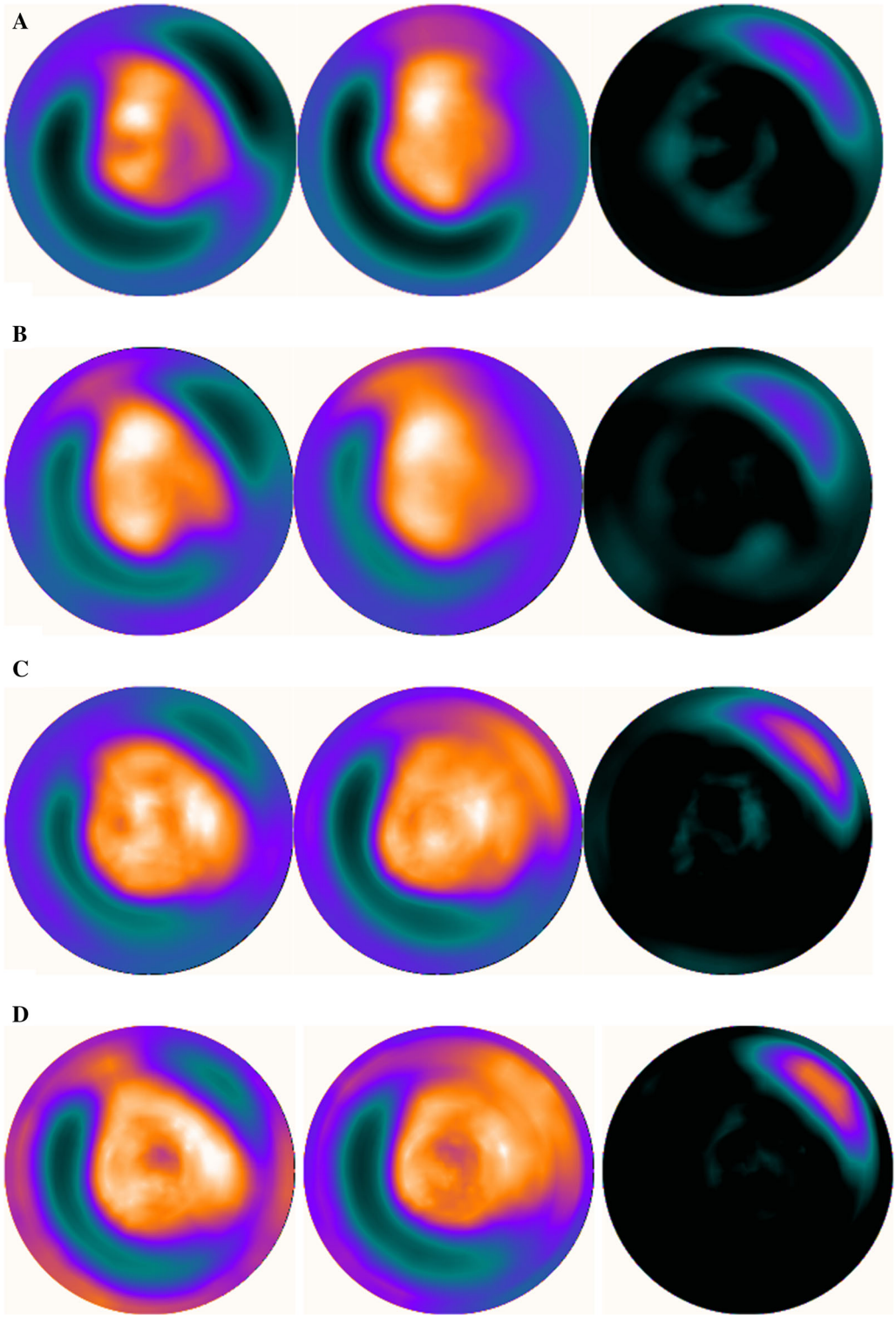

Figure 5. Single-isotope (separate ^{123}I and ^{99m}Tc) acquisitions and mismatch on DNM 530c (**A**) and DSPECT (**C**) and simultaneous dual-isotope (^{123}I and ^{99m}Tc) acquisitions and mismatch on DNM 530c (**B**) and DSPECT (**D**) presented as the bull's eye polar maps of the 22-min acquisitions.

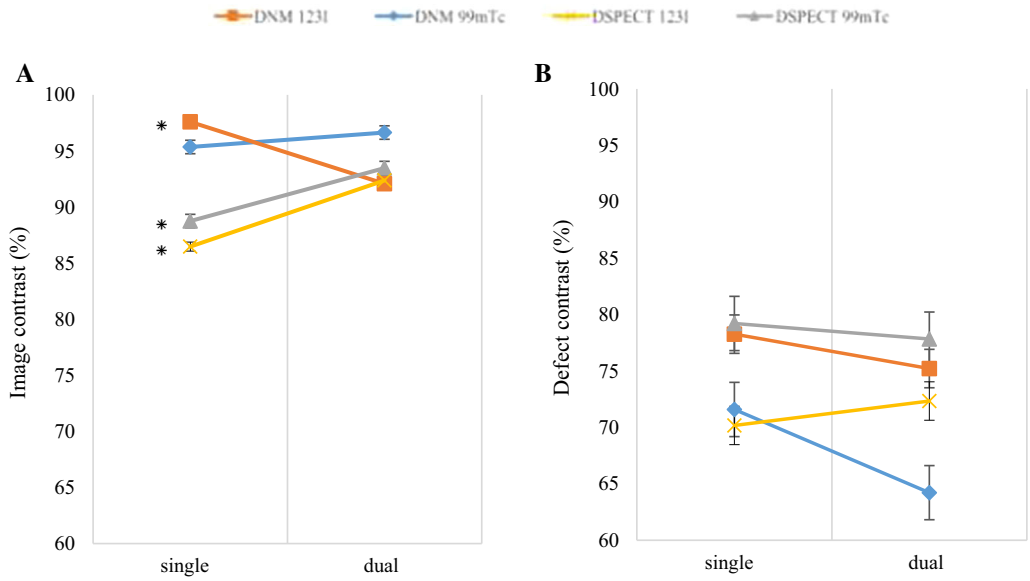

Figure 6. Image (**A**) and defect (**B**) contrasts with single (separate ^{123}I and ^{99m}Tc) acquisitions compared with simultaneous dual-isotope (^{123}I and ^{99m}Tc) acquisitions for both energy windows (^{123}I and ^{99m}Tc) on DNM 530c and DSPECT expressed as mean value ± standard deviation. *$P < .0001$ vs dual.

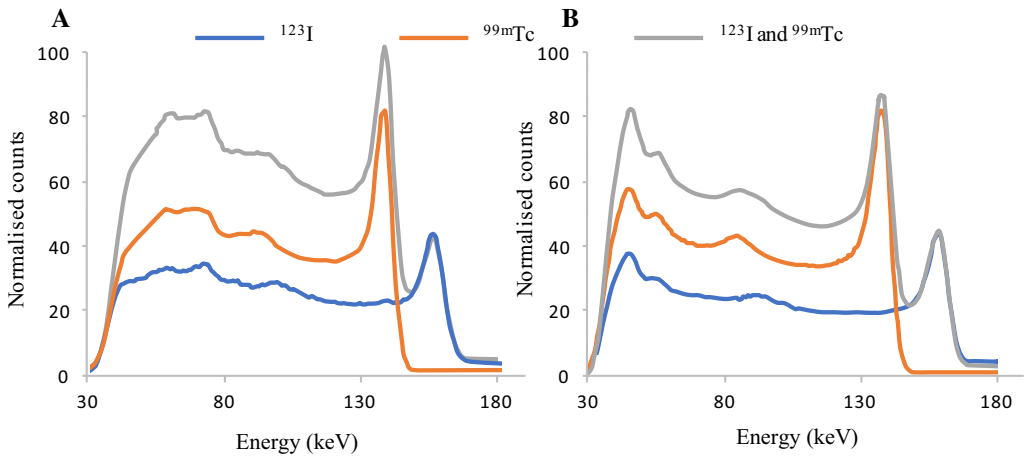

Figure 7. Single-isotope (separate ^{123}I and ^{99m}Tc) and simultaneous dual-isotope (^{123}I and ^{99m}Tc) acquisitions on DNM 530c (**A**) and DSPECT (**B**) presented as the energy spectra of the 7-min acquisitions.

NEW KNOWLEDGE GAINED

With an increased energy resolution, the CZT cameras may allow, under routine conditions, a simultaneous and accurate segmental study of myocardial innervation and perfusion (match and mismatch).

CONCLUSION

In this phantom study, the two CZT cameras (DNM 530c and DSPECT) provided similar results in the evaluation of regional myocardial innervation and perfusion match and mismatch with single- (separate ^{123}I

and ^{99m}Tc acquisitions) and simultaneous dual-isotope (^{123}I and ^{99m}Tc) acquisitions. These findings may have diagnostic and therapeutic implications in heart failure patients referred for a combined assessment of perfusion and innervation.

Acknowledgment

Nathaniel Roth, Rafael Baavour, Sylvie Petit, Mathilde Thélu, and the nuclear medicine technicians at Caen and Lille for their technical assistance.

Disclosures

The authors have indicated that they have no financial conflict of interest.

References

1. Zipes DP (1991) Sympathetic stimulation and arrhythmias. N Engl J Med 325:656-657
2. Carrio I, Cowie MR, Yamazaki J, Udelson J, Camici PG (2010) Cardiac sympathetic imaging with mIBG in heart failure. JACC Cardiovasc Imaging 3:92-100
3. Morozumi T, Kusuoka H, Fukuchi K, Tani A, Uehara T, Matsuda S et al (1997) Myocardial iodine-123-metaiodobenzylguanidine images and autonomic nerve activity in normal subjects. J Nucl Med 38:49-52
4. Merlet P, Benvenuti C, Moyse D, Pouillart F, Dubois-Rande JL, Duval AM et al (1999) Prognostic value of MIBG imaging in idiopathic dilated cardiomyopathy. J Nucl Med 40:917-923
5. Manrique A, Bernard M, Hitzel A, Bauer F, Menard JF, Sabatier R et al (2008) Prognostic value of sympathetic innervation and cardiac asynchrony in dilated cardiomyopathy. Eur J Nucl Med Mol Imaging 35:2074-2081
6. Jacobson AF, Senior R, Cerqueira MD, Wong ND, Thomas GS, Lopez VA et al (2010) Myocardial iodine-123 meta-iodobenzylguanidine imaging and cardiac events in heart failure. Results of the prospective ADMIRE-HF (AdreView Myocardial Imaging for Risk Evaluation in Heart Failure) study. J Am Coll Cardiol 55:2212-2221
7. Agostini D, Marie PY, Ben-Haim S, Rouzet F, Songy B, Giordano A et al (2016) Performance of cardiac cadmium-zinc-telluride gamma camera imaging in coronary artery disease: A review from the cardiovascular committee of the European Association of Nuclear Medicine (EANM). Eur J Nucl Med Mol Imaging 43:2423-2432
8. Gimelli A, Liga R, Genovesi D, Giorgetti A, Kusch A, Marzullo P (2014) Association between left ventricular regional sympathetic denervation and mechanical dyssynchrony in phase analysis: A cardiac CZT study. Eur J Nucl Med Mol Imaging 41:946-955
9. Gimelli A, Liga R, Giorgetti A, Genovesi D, Marzullo P (2014) Assessment of myocardial adrenergic innervation with a solid-state dedicated cardiac cadmium-zinc-telluride camera: First clinical experience. Eur Heart J Cardiovasc Imaging 15:575-585
10. Tinti E, Positano V, Giorgetti A, Marzullo P (2014) Feasibility of [(123)I]-meta-iodobenzylguanidine dynamic 3-D kinetic analysis in vivo using a CZT ultrafast camera: Preliminary results. Eur J Nucl Med Mol Imaging 41:167-173
11. Bellevre D, Manrique A, Legallois D, Bross S, Baavour R, Roth N et al (2015) First determination of the heart-to-mediastinum ratio using cardiac dual isotope (123I-MIBG/99mTc-tetrofosmin) CZT imaging in patients with heart failure: The ADRECARD study. Eur J Nucl Med Mol Imaging 42:1912-1919
12. Cochet H, Bullier E, Gerbaud E, Durieux M, Godbert Y, Lederlin M et al (2013) Absolute quantification of left ventricular global and regional function at nuclear MPI using ultrafast CZT SPECT: Initial validation versus cardiac MR. J Nucl Med 54:556-563
13. Bailliez A, Blaire T, Mouquet F, Legghe R, Etienne B, Legallois D et al (2014) Segmental and global left ventricular function assessment using gated SPECT with a semiconductor Cadmium Zinc Telluride (CZT) camera: Phantom study and clinical validation vs cardiac magnetic resonance. J Nucl Cardiol 21:712-722
14. Bailliez A, Lairez O, Merlin C, Piriou N, Legallois D, Blaire T et al (2016) Left ventricular function assessment using 2 different cadmium-zinc-telluride cameras compared with a gamma-camera with cardiofocal collimators: Dynamic cardiac phantom study and clinical validation. J Nucl Med 57:1370-1375
15. Verberne HJ, Acampa W, Anagnostopoulos C, Ballinger J, Bengel F, De Bondt P et al (2015) EANM procedural guidelines for radionuclide myocardial perfusion imaging with SPECT and SPECT/CT: 2015 revision. Eur J Nucl Med Mol Imaging 42:1929-1940
16. Erlandsson K, Kacperski K, van Gramberg D, Hutton BF (2009) Performance evaluation of D-SPECT: A novel SPECT system for nuclear cardiology. Phys Med Biol 54:2635-2649
17. Leo W (1994) Techniques for nuclear and particle physics experiments, 2nd edn. Spinger, Berlin
18. Verberne HJ, Feenstra C, de Jong WM, Somsen GA, van Eck-Smit BL, Busemann Sokole E (2005) Influence of collimator choice and simulated clinical conditions on 123I-MIBG heart/mediastinum ratios: A phantom study. Eur J Nucl Med Mol Imaging 32:1100-1107
19. Bocher M, Blevis IM, Tsukerman L, Shrem Y, Kovalski G, Volokh L (2010) A fast cardiac gamma camera with dynamic SPECT capabilities: Design, system validation and future potential. Eur J Nucl Med Mol Imaging 37:1887-1902
20. Kacperski K, Erlandsson K, Ben-Haim S, Hutton BF (2011) Iterative deconvolution of simultaneous 99mTc and 201Tl projection data measured on a CdZnTe-based cardiac SPECT scanner. Phys Med Biol 56:1397-1414
21. Berman DS, Kang X, Gransar H, Gerlach J, Friedman JD, Hayes SW et al (2009) Quantitative assessment of myocardial perfusion abnormality on SPECT myocardial perfusion imaging is more reproducible than expert visual analysis. J Nucl Cardiol 16:45-53
22. Schneider CA, Rasband WS, Eliceiri KW (2012) NIH Image to ImageJ: 25 years of image analysis. Nat Methods 9:671-675
23. Morgan CJ, Aban I (2016) Methods for evaluating the agreement between diagnostic tests. J Nucl Cardiol 23:511-513
24. Bland JM, Altman DG (1986) Statistical methods for assessing agreement between two methods of clinical measurement. Lancet 1:307-310
25. Kumita S, Cho K, Nakajo H, Toba M, Kijima T, Mizumura S et al (2000) Simultaneous assessment of Tc-99m-sestamibi and I-123-BMIPP myocardial distribution in patients with myocardial infarction: Evaluation of left ventricular function with ECG-gated myocardial SPECT. Ann Nucl Med 14:453-459
26. Ouyang J, Zhu X, Trott CM, El Fakhri G (2009) Quantitative simultaneous 99mTc/123I cardiac SPECT using MC-JOSEM. Med Phys 36:602-611
27. Flotats A, Carrio I, Agostini D, Le Guludec D, Marcassa C, Schafers M et al (2010) Proposal for standardization of 123I-metaiodobenzylguanidine (MIBG) cardiac sympathetic imaging

by the EANM Cardiovascular Committee and the European Council of Nuclear Cardiology. Eur J Nucl Med Mol Imaging 37:1802-1812

28. Abdulghani M, Duell J, Smith M, Chen W, Bentzen SM, Asoglu R et al (2015) Global and regional myocardial innervation before and after ablation of drug-refractory ventricular tachycardia assessed with 123I-MIBG. J Nucl Med 56(Suppl 4):52S-58S
29. Fan P, Hutton BF, Holstensson M, Ljungberg M, Hendrik Pretorius P, Prasad R et al (2015) Scatter and crosstalk corrections for (99m)Tc/(123)I dual-radionuclide imaging using a CZT SPECT system with pinhole collimators. Med Phys 42:6895
30. Holstensson M, Erlandsson K, Poludniowski G, Ben-Haim S, Hutton BF (2015) Model-based correction for scatter and tailing effects in simultaneous 99mTc and 123I imaging for a CdZnTe cardiac SPECT camera. Phys Med Biol 60:3045-3063
31. D'Estanque E, Hedon C, Lattuca B, Bourdon A, Benkiran M, Verd A et al (2016) Optimization of a simultaneous dual-isotope 201Tl/123I-MIBG myocardial SPECT imaging protocol with a CZT camera for trigger zone assessment after myocardial infarction for routine clinical settings: Are delayed acquisition and scatter correction necessary? J Nucl Cardiol. doi:10.1007/s12350-016-0524-1